Available online at www.sciencedirect.com

ScienceDirect

IFAC Papers Online CONFERENCE PAPER ARCHIVE

IFAC PapersOnLine 50-1 (2017) 11479–11484

Exploring Robots and UAVs as Phenotyping Tools in Plant Breeding

Ingunn Burud * **Gunnar Lange** * **Morten Lillemo** **
Eivind Bleken * **Lars Grimstad** * **Pål Johan From** *

* *Faculty of Sciences and Technology, Norwegian University of Life Sciences*

** *Department of Plant Sciences, Norwegian University of Life Sciences*

Abstract: Recent advances in robot and sensor technology makes it possible to survey a large number of plants in a non destructive and cost efficient way. The present research approach includes measurements with VIS/NIR multispectral camera mounted on UAV and robot and traditional manual ground measurements. The analysis presented here, aims (1) to evaluate the use of multispectral imaging from drone and robot as phenotyping tools, (2) to compare images from drone and robot to see how they can complement each other for an optimized analysis of the plants and (3) to study the reflectance response of various plant species exposed to two different regimes of fertilizers. The sensors on UAVs provide a unique perspective of the growth of the plants revealing the map of the variations within the field of study.

© 2017, IFAC (International Federation of Automatic Control) Hosting by Elsevier Ltd. All rights reserved.

Keywords: multi-sensor systems, mobile robots, UAVs, agricultural robotics

1. INTRODUCTION

New approaches are necessary to meet the goals of increased food production. Plant breeding can play a key role by developing cultivars with higher yield potential and better adaptation to stress. Progress in breeding depends on the ability to design crosses with complementary traits, and then perform effective selection among the offspring. This requires precise and cost-effective methods to evaluate large numbers of plants across relevant environments and stresses. Traditional data capture based on low throughput and manual methods is labour-intensive and prone to human errors. While the costs of sequencing and genotyping have dropped dramatically over the last decade, the labour cost has increased and phenotyping has now become the biggest bottleneck for realizing the full potential of genomics in plant breeding.

The reflectance of electromagnetic energy by the crop canopy at different wavelengths is predictive of important physiological traits such as leaf nitrogen content, photosynthetically active biomass, leaf chlorophyll and plant water status. Direct measurements are closely associated with grain yield, but destructive and time consuming. Canopy reflectance may therefore replace traditional methods to screen large numbers of field plots in a fast and cost-effective manner. Spectral measurements have traditionally been obtained using hand-held or tractor-mounted sensors (Andrade-Sanchez et al., 2014), but multispectral imaging now offers the possibility to combine spectral radiation with spatial information and thus perform a simultaneous phenotyping of both the physical structure and physiological conditions of plants (Araus and Cairns 2014). Even a simple RGB camera can be used to extract parameters related to biomass and plant physiological status, but more information can be obtained by multispectral and hyperspectral cameras that include a larger proportion of the electromagnetic spectrum. Some wavelengths contain more biologically relevant information than others, and several spectral indices like the NDVI (normalized differential vegetation index) and EVI (enhanced vegetation index) are widely used.

These recent advances in machine vision and imaging have resulted in several new robotic systems developed for high-throughput phenotyping. Autonomous ground robots have been developed for information gathering, such as Bonirob (V2) (Bangert et al., 2013), the RIPPA (Robot for Intelligent Perception and Precision Application) from University of Sydney and the Thorvald robot used in this work (Grimstad et al., 2015). Airborne cameras have also gained much interest. In particular, UAVs and autononomous aircrafts have been used both commercially and in several different research projects (Chapman et al., 2014). The Flourish project aims at combining the aerial survey capabilities of a small autonomous multi-copter UAV with a multi-purpose agricultural Unmanned Ground Vehicle (UGV) (Liebisch et al., 2016), taking advantage of the main positive aspects of each system.

A strategic collaboration has been initiated at the Norwegian University of Life Sciences, where research groups across departments and disciplines are joining forces to explore how multispectral imaging can be used as a phenotyping technology in plant breeding research. This includes the development and testing of multispectral imaging in visible and near infrared wavelengths of plants in field trials, using cameras mounted on an autonomous field robot and on an Unmanned Airborne Vehicle (UAV). This equipment is part of a common sensor lab that has been established at the university, which also serves many other research purposes. Based on pilot projects run during

2405-8963 © 2017, IFAC (International Federation of Automatic Control) Hosting by Elsevier Ltd. All rights reserved.
Peer review under responsibility of International Federation of Automatic Control.
10.1016/j.ifacol.2017.08.1591

the summer of 2016 there are plans to upgrade the field research station with new facilities for high-throughput field phenotyping. Examples of ongoing research and some preliminary results from the pilot project comparing the use of robot and drones in field trials are presented.

2. MATERIAL AND METHODS

2.1 Study site

A set of 24 spring wheat cultivars and breeding lines representing the yield progress over the last 40 years in Norway (Lillemo and Dieseth., 2011) was planted in a yield trial at Vollebekk research station in Ås, south-eastern Norway. Two nitrogen (N) fertilization levels were applied: 75 and 150 kg N/ha (named high-N and low-N hereafter) representing the typical N fertilization levels of the 1970s and today. The trial was laid out in an alpha-lattice split plot design with two reps of each variety within each N-level as displayed in Fig. 1. . The trial was planted on May 12, using a seeding rate of 23 g/m2. The plots were 1.5 m wide and 4 m long, and with a 1 m alley between plots. The trial was treated with herbicides and fungicides following normal agronomic practice in order to get a true measure of grain yield in the absence of any biotic stress. The following traits were measured manually during the growing season: heading date, maturity date and plant height. Heading is the phase in the plant development when a head emerges from the sheath of the upper leaf. When all plants had matured, the whole trial was harvested using a plot combine. The samples were weighed to calculate grain yield, and the samples were analysed to obtain standard grain quality parameters 1000-kernel weight, hectoliter weight and protein content.

2.2 Robotic System

The robot used in this work is the Thorvald I agricultural platform. The robot is powerful enough to perform energy-demanding operations as well as possessing the beneficial properties of lightweight, autonomous robots. The Thorvald platform was designed and built at the Norwegian University of Life Sciences. It has a low center of gravity, and a total mass of approx. 150 kg. For monitoring and surveillance, the robot is sufficiently light weight not to damage the plants and the soil and to maintain a long operation time. The robot has individual steering motors for each wheel, which makes it highly maneuverable, and the frame members and frame joints are made somewhat flexible to ensure that all wheels will remain in contact with the ground, even in rough terrain. The robot is depicted in Fig. 2.

In addition to the ground vehicle, a UAV was also used to obtain remote images covering the whole field. A DJI Phantom3 drone was used, that can carry small payloads such as light-weight cameras. The drone was pre-programmed to take several pictures of the entire field and the pictures were then post-processed and stitched together to make a complete map of the field.

2.3 Imaging

The research approach considered in this study included measurements with a multispectral camera with three

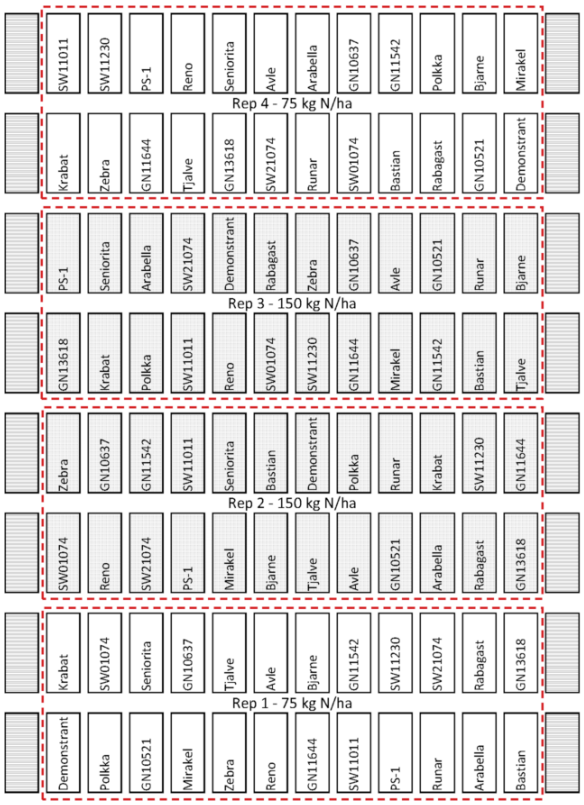

Fig. 1. Map of the 24 spring cultivars laid out in an alpha-lattice split plot design with two reps of each variety within each N-level

Fig. 2. The Thorvald I robot used for the field tests

broad band spectral channels: green, red and near infrared (NIR), one narrow band channel and an RGB sensor (Parrot Sequoia, Micasence.com). The wavebands for the four sensor bands of the Parrot Sequoia camera are shown together with typical reflectance spectra of a healthy and a stressed plant in Fig. 3. As can be seen on the figure, healthy vegetation reflects a very high amount of the solar radiation in the NIR part of the electromagnetic spectrum. These wavelengths can not be seen by the human eye, which is why the plants look green to humans, as there is a small increase in the reflection in the green part of the

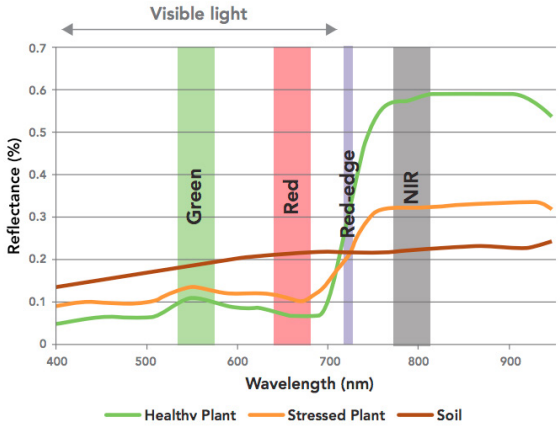

Fig. 3. Typical reflectance spectra of soil, a healthy and a stressed plant, with wavebands of the Parrot Sequoia camera (Micasence.com)

visible wavelengths. The NIR sensor on the camera can detect the NIR reflection of the plants and the relation between the NIR reflectance and the red band reflectance indicate something about the health of a plant. In order to compute the reflectance in all the bands independent of the light conditions of the moment of the measurement a standardized white calibration plate reflecting 100% of the solar radiation was recorded before each set of images and a sunshine sensor connected to the camera corrected for varying light conditions during the measurements. The camera was mounted both on the UAV and the robot. On the robot the camera was attached to a rack with fixed distance to the ground, the camera looking down on the plots (at nadir). The sunshine sensor was placed on top of the rack. The robot was programmed to drive along each of the 14 plot rows taking 2 images of each plot. On the UAV the camera was attached underneath the drone and the sunshine sensor on top. The camera was programmed to record images at regular time intervals during the flight. The UAV was programmed to fly over the field at a fixed height of 15m above ground, in straight lines and with constant speed taking regular images in order to cover the whole field.

2.4 Data analysis

The multispectral images obtained from the UAV were first uploaded to the Atlas software (Micasence.com) where the individual frames were stitched together to a map. The algorithm uses a combination of GPS cordinates and image features to stitch the images correctly together. The software outputs a map in each of the wavelength bands: green, red, NIR and narrow band. In addition a digital elevation map is generated, which is a 3D representation of the terrain (Li et al., 2005). These are georeferenced images and can be integrated directly into a map of the area (e.g. Google map). The georeferenced multispectral images were then further analysed using selfwritten scripts in the Python software. Maps of the NDVI were computed as a subtraction of the red reflectance values from the NIR, divided by the sum of NIR and red bands according to the equation (1):

$$NDVI = \frac{NIR - R}{NIR + R}, \tag{1}$$

where NIR and R are the reflectance values in the near infrared and red wavebands, respectively. The values of NDVI goes from -1 to 1 and values for vegetation are generally between 0.4 and 1.

Mean values of NDVI for each individual plot were also computed. The images from the different dates were first aligned due to slightly different orientations and resolution. In some cases the GPS signals to the UAV were unstable and we had to fly manually over the field which resulted in some maps that did not have full coverage of all plots. The alignment was carried out by using a combination of GPS coordinates, and an alignment procedure using a minimum of 4 manually selected reference points. An automatic edge detection of the plots was complex due to the varying edges of the plots during the growth period of the plants. Thererfore, a manual selection of the plots was carried out on one of the maps and given that all the maps were aligned, this selection could be used further on all the maps automatically. In this way, values of all the plots of all dates coul be computed automatically, once the selection of the first plot was performed. Only the inner part of each plot was selected in order to minimize errors due to edges of plots or small alignment errors. In order not to include values from soil, all the NDVI values below 0.3 were removed and not included in the analysis.

The DEM frames were used to compute the mean height for each plot. A background correction of the height variations in the ground was performed by selecting small regions around the field and between the plots, computing the mean values of these regions and then performing a regression in two directions (x,y) along the rows and columns of the plots. The modelled background values was subtracted from the respective mean height value of each plot.

The images from the robot were read individually into the computer programme and the mean NDVI values of each plot was computed as the mean of the two images obtained. This could be done automatically as the robot always followed the same route through the plots with two images per plot.

3. RESULTS AND DISCUSSION

3.1 Robotic system

During the experiments with the robot, several interesting observations were made. Firstly, the width of the wheels needed to be narrower, as they touched the wheat as the robot was moving in the field. Secondly, as the crop grew higher, the relatively low ground clearance of only 59 cm made the robot bend the crop, which was becoming increasingly troubling with higher crop. It was also noticed that it would be nice to be able to change the width of the robot itself, as the track sizes of the different field experiments were different. It was therefore decided to build a second robot, the Thorvald II. This robot has narrower wheels, a ground clearance of up to 180 cm, and is completely modular so that it can be re-configured into a wide variety of designs and widths using only

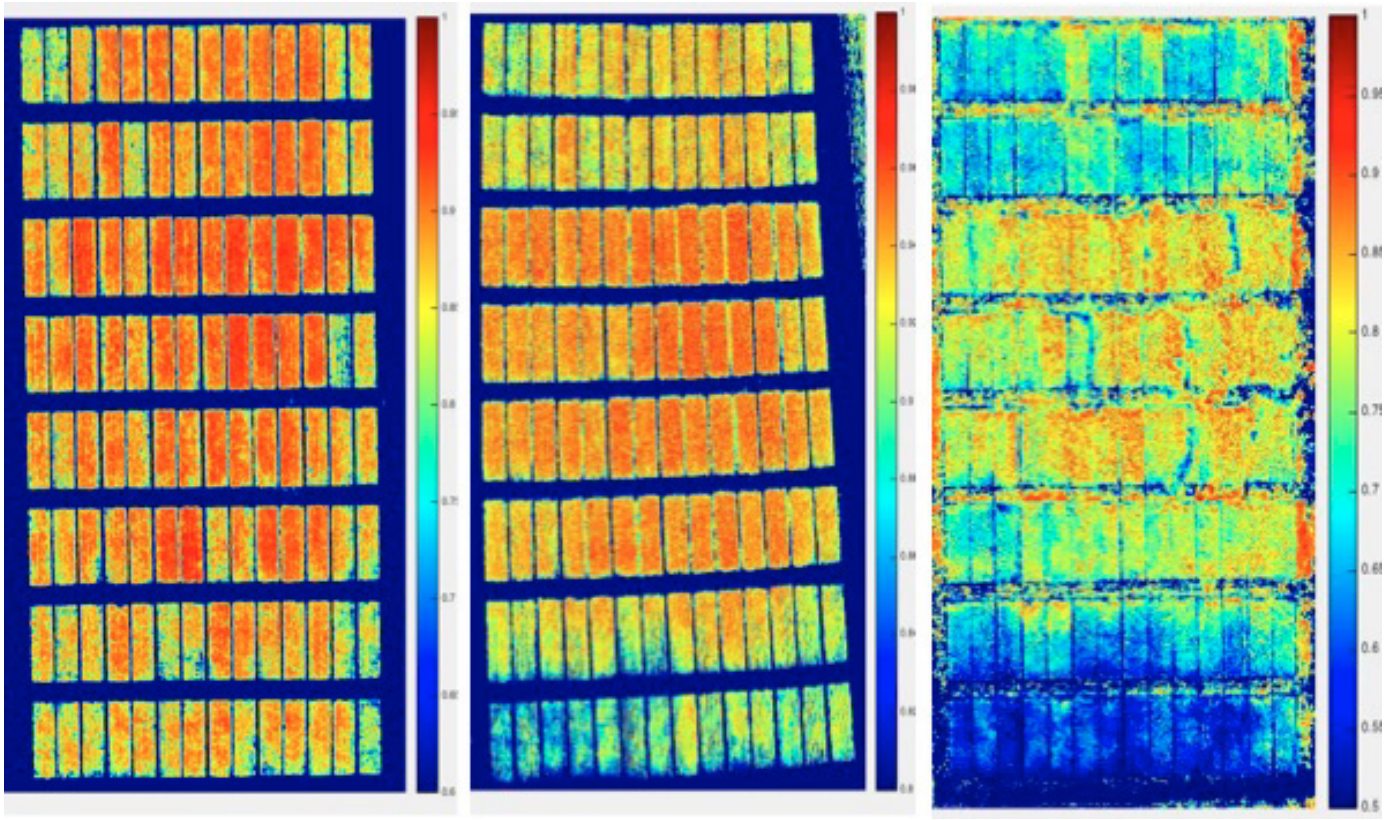

Fig. 4. NDVI map of the field from left to right 17.06.2016, 18.07.2016 and 10.08.2016

Fig. 5. The Thorvald II robot specifically designed for phenotyping tasks, with narrower wheels, higher ground clearance, and a modular design allowing us to rebuild the robot into a wide variety of configurations and sizes.

standard hand tools. The robot is illustrated in Fig. 5 and is described in detail in Grimstad and From (2017).

3.2 Agricultural measurements

Three NDVI maps obtained from the UAV from different dates, 17.06, 18.07 and 10.08 are shown in Fig. 4. There are several observations to be pointed out from these maps: i) There are large variations in the field along the growth season. The NDVI values on the 17.06 have already reached high values for most of the plots, they have decreased slightly but remain high on the 18.07 and have decreased considerably on the map from 10.08. ii) There is a large variation between the plots, and in particular it can be noticed that the NDVI for the four middle blocks are generally higher than for the outer blocks. This is expected since these blocks recieved a higher dose of Nitrogen (high-N) than the outer rows (low-N). iii) The NDVI for the plants exposed to high Nitrogen fertilization remains higher towards the end of the growth period than for the plants exposed to low Nitrogen fertilization. iv) The last image from 10.08 is influenced by lodging of the plots with long and weak straws.

The time series of the mean NDVI values for some selected plots are shown in Fig. 6. We selected the plots that had full coverage for all the measurement dates. The start time (day 0) on the figure indicates the date 17.06. The NDVI clearly increases with time and remains at a high plateu value for a time period of approximately 15 days. The highest values for the plots exposed to low-N has a mean value of 0.92 whereas the mean value for the plots exposed to high-N is of 0.95. This is also clearly seen on the maps (Fig. 4). From day 30 to day 60 the NDVI value decreases rapidly for the plots exposed to low-N. For the plots exposed to high-N the NDVI remains high up to day 50 and decreases towards day 60 as the grains ripen. The NDVI values are generally believed to be related to the yield of crops, which was also confirmed in this study. The mean value of the measured yield for all the low-N plots was 528.8 kg/daa versus 680.9 kg/daa for the high-N plots. This agrees with the mean NDVI measured for the low-N and high-N plots.

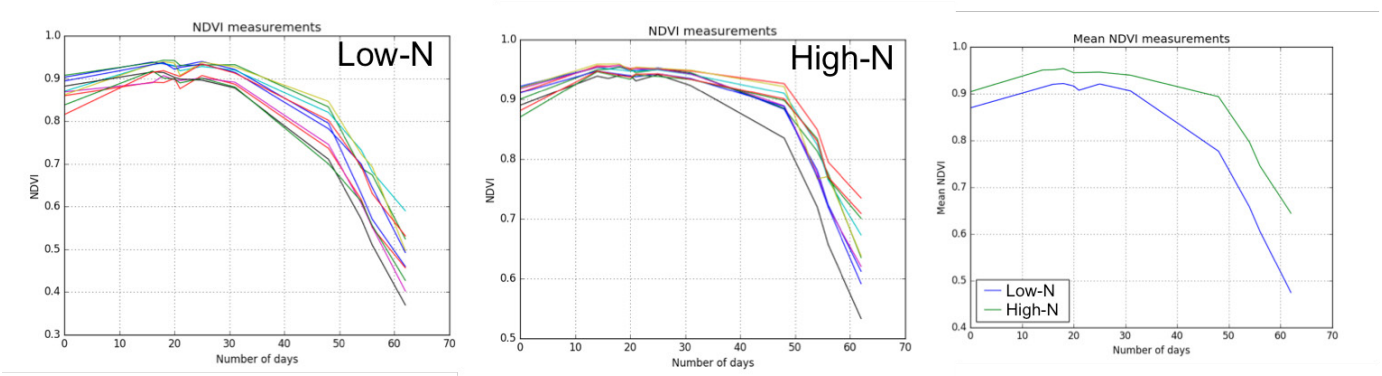

Fig. 6. NDVI time curves of selected plots exposed to low-N (left), High-N (middle) and mean value of low and high Nitrogen exposure.

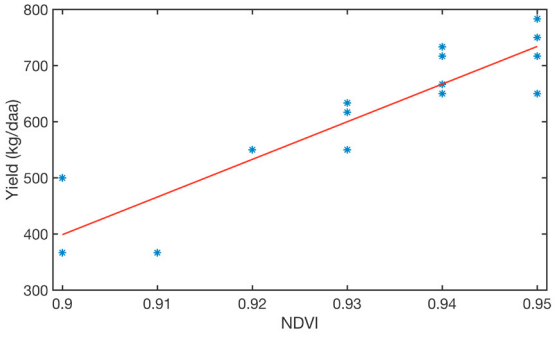

Fig. 7. Measurement of maximum NDVI vlaues from drone images versus ground measurements of yield for some of the plots (Mirakel, Bjarne, Demonstrant, SNW1101) with good time coverage was obtained.

The maximum NDVI measurement for some of the wheat cultivars (Mirakel, Demonstrant, SW1101 and Bjarne) were compared with their respective yield measurement, which is displayed in Fig. 7. A linear fit to the data points is also shown in the figure. There is a clear correlation between the maximum NDVI values and the yield. When comparing the NDVI curves with the heading dates from ground measurement we note that the heading occurs at the beginning of the maximum plateau of the NDVI curve for all the plots and treatments. For all the curves there seems to be a small dip in the curve just after heading, however, this needs to be confirmed in further studies. There does not seem to be any difference between the two treatments (low-N and high-N) regarding the maximum reach of the NDVI and hence the heading dates from the NDVI curves, which is confirmed by the manual ground measurements: day 18.3 on the curve for low-N and day 18.7 for high-N.

An additional output from the processing of the drone images is the 3D model of the field in a DEM which makes it possible to estimate the height of the plants, as shown in the visualisation of the plot for the date 18.07 in Fig. 8. It can be seen from the map that the mean plant height varies for the plots across the field. The estimated heights from July 18th were compared with the manually measured heights from end of July and a correlation of 0.68 was found between them.

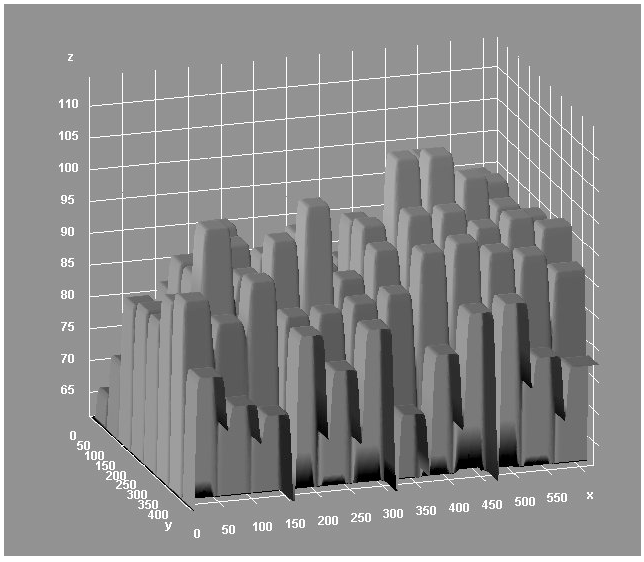

Fig. 8. Mean height of each plot dervied from the Digital Elevation Map of the field from the stitched drone images from 18.07. The z-axis shows the height of the plots.

The robot images from the start of the growth season contain a few plants close to the ground. However, during the growth season the plants grow higher, and since the height of the robot was fixed during this survey the growing plants reached too close to the robot and the camera. This was both destructive for the plants and influenced the images. Since the images were obtained from nadir they suffered from a few very exposed points at the top of the plants and shadowed parts underneath. The sunshine sensor did not perform as expcted in these conditions and many of the images were saturated and could not be white reference calibrated. Towards the end of the season an updated firmware was installed for the sunshine sensor, which improved the results from the robot images. The NDVI values computed automatically from the robot images showed a big decrease in NDVI around the moment of heading, then an increase. Due to uncertainties around the saturation, calibration and shadow effects of the lower parts of the plants these NDVI values were not used in the analysis of the plots. Examples of images from the 6 dates during the growth season, 27.05, 16.06, 28.06, 03.07, 18.07 and 04.08 are displayed in Fig. 9

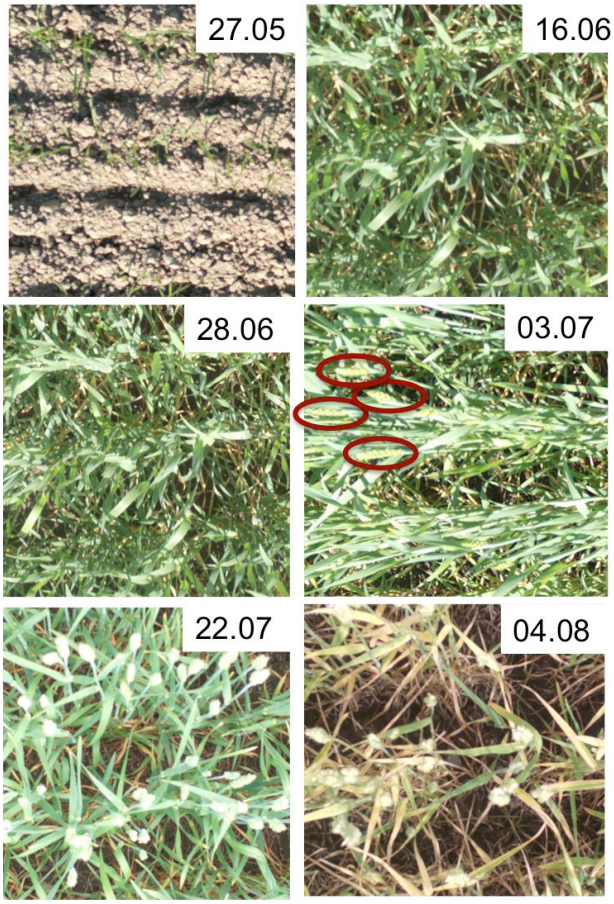

Fig. 9. Close up of robot images of the cultivar Mirakel exposed to low-N from different dates during the growth season. The heading at 03.07 is indicated with the purple ovals.

for the cultivar called Mirakel exposed to 8 kg of fertilizer. Sections of the whole images are extracted to show details of the plants. It can be seen that no heading is present on the image of 28.06 and that it has occured on the image from 03.07, which agrees with the manual ground measurements of the heading date that was also noted to be 03.07. Possibly the detection of heading could be done automatically on the images from the robot by spectral analysis or spatial pattern recognition.

It is clear that the images from the drone and the robot did not provide the same information in this survey. Whereas the NDVI maps from the drone provide indications on the yield and time of heading, robot images obtained closer to the plants could be used to study close up features of the plants. In order to get reliable NDVI measurements also from the robot, two cameras at different angles could be used, one at nadir and one at e.g., 50 degrees. The images obtained at the 50 degrees angle will be able to capture larger parts of the plants. This is especially true in the case where the plants have grown high, and the nadir images will only measure the surface covering the ground.

4. CONCLUSION

The integration of multispectral sensors on UAV and robot provides an enhanced and flexible measured survey solution with accurate data captured on site. The calibrated NDVI images obtained by aerial sensing confirm the measurements carried out at ground level and could be used to compute heading dates and yield estimate. Sensors and methods developed for UAVs are not directly applicable for ground robots. However, the images from the robot display close details of the plants that can be explored further by the means of advanced image analysis. In future works one would like to expand the sensors to hyperspectral camera. Pre-defined spectral indices such as NDVI might lead to an over-simplified or even misleading interpretation as they consider only a few distinct wavelengths. By covering a wider spectral range with high spatial resolution up to centimeters, the new measurement capabilities with the integrated methodology will advance the prediction accuracy of different traits of the plants.

ACKNOWLEDGEMENTS

The project was supported by a scholarship from Yara Norge and strategic funds provided by the Norwegian University of Life Sciences.

REFERENCES

Andrade-Sanchez, P., Gore, M., Heun, J., Thorp, K., Carmo-Silva, A., French, A., Salvucc, i.M., and White, J. (2014). Development and evaluation of a field-based high-throughput phenotyping platform. *Functional Plant Biology*, 41, 68–79.

Bangert, W., Kielhorn, A., Rahe, F., Albert, A., Biber, P., Grzonka, S., Haug, S., Michaels, A., Mentrup, D., Hänsel, M., et al. (2013). Field-robot-based agriculture:remotefarming. 1 and bonirob-apps. In *71th conference LAND. TECHNIK-AgEng 2013*, 439–446.

Chapman, S., Merz, T., Chan, A., Jackway, P., Hrabar, S., Dreccer, M., and et al. (2014). Pheno-copter: a low-altitude, autonomous remote-sensing robotic helicopter for high-throughput field-based phenotyping. *Agronomy*, 4, 279–301.

Grimstad, L. and From, P.J. (2017). Thorvald ii - a modular and re-configurable agricultural robot. In *IFAC 2017 World Congress, 2017*.

Grimstad, L., Phan, H.N.T., Pham, C.D., Bjugstad, N., and From, P.J. (2015). Initial feld-testing of thorvald - a versatile robotic platform for agricultural applications. In *IROS Workshop on Agri-Food Robotics: dealing with natural variability, 2015*.

Li, Z., Zhu, Q., and Gold, C. (2005). *Digital Terrain Modeling: Principles and Methodology*. CRC Press.

Liebisch, F., Pfeifer, J., Khanna, R., Lottes, P., Stachniss, C., Falck, T., Sander, S., Siegwart, R., Walter, A., and Galceran, E. (2016). Flourish-a robotic approach for automation in crop management. In *Workshop Computer-Bildanalyse und Unbemannte autonom fliegende Systeme in der Landwirtschaft, 2016*.

Lillemo, M. and Dieseth., J. (2011). Wheat breeding in norway. *A. P. Bonjean, W. J. Angus and M. van Ginkel, editors, The World Wheat Book. A history of wheat breeding.*, 2, 45–79.